國立臺灣大學電機資訊學院生醫電子與資訊學研究所
博士論文
Graduate Institute of Biomedical Electronics and Bioinformatics
College of Electrical Engineering and Computer Science
National Taiwan University
Doctoral Dissertation

利用葡萄糖正子掃描評估早期治療反應來預測
轉移性肺腺癌病患接受得紓緩標靶藥物之預後

FDG-PET in early response assessment for predicting
outcomes in patients with metastatic lung adenocarcinoma
treated with erlotinib

何恭之
Kung-Chu Ho

指導教授：鍾孝文 教授
Advisor: Hsiao-Wen Chung, Prof.

中華民國 105 年 12 月
Dec. 2016

國立臺灣大學 博士學位論文
口試委員會審定書

利用葡萄糖正子掃描評估早期治療反應來預測
轉移性肺腺癌病患接受得紓緩標靶藥物之預後

FDG-PET in early response assessment for predicting outcomes in patients with metastatic lung adenocarcinoma treated with erlotinib

本論文係 何恭之 君（學號 D98945005）在國立臺灣大學生醫電子與資訊學研究所完成之博士學位論文，於民國 105 年 12 月 09 日承下列考試委員審查通過及口試及格，特此證明

口試委員：

_____（簽名）

（指導教授）

系主任、所長 _____（簽名）

中文摘要

目的: 本研究在探討利用葡萄糖正子掃描評估轉移性肺腺癌接受得紓緩標靶藥物治療之早期反應，以 TLG-S 方法是否比 EORTC 標準與 PERCIST 標準更能有效預測病患之預後。此研究的假設是源自於原發腫瘤與轉移腫瘤的生物特性差異以及骨骼顯像上的復燃現象。此外，腫瘤影像上的紋理特性對於疾病預後的價值也進行探討。

方法: 我們回溯性分析前瞻性收集的 23 位接受得紓緩治療之轉移性肺腺癌病患。每位受試者都接受葡萄糖正子掃描於給藥前，給藥第 14 日，與給藥第 56 日。診斷性電腦斷層於給藥前與給藥第 56 日施行。葡萄糖正子掃描的反應評估利用 TLG-S、EORTC 與 PERCIST 標準進行。電腦斷層的 RECIST 1.1 標準作為治療反應的比較基準。影像紋理特性分析了 coarseness、contrast、busyness、complexity 與 strength 參數。兩年無惡化存活期與整體存活期作為疾病預後的評估指標。

結果: 我們發現 13 位病患有骨骼轉移。其中 4 位(31%)在給藥第 14 日有發生骨骼顯像上的復燃現象，依據 PERCIST 標準被誤判為藥物不反應組。依據給藥第 14 日 TLG-S 標準被歸為藥物有反應組之病患，擁有較高的兩年無惡化存活期(26.7% vs. 0%, $P = 0.007$) 與整體存活期(40.0% vs. 7.7%, $P = 0.018$)。依據給藥第 56 日電腦斷層 RECIST 標準也呈現相同的存活期。依據給藥第 14 日 EORTC 標準被歸為藥物有反應組之病患，擁有較高的兩年整體存活期(36.4% vs. 8.3%, $P = 0.015$)。早期 busyness 參數的變化在無惡化存活期有顯著意義($P = 0.004$) 且早期 coarseness 參數的變化在無惡化存活期($P = 0.007$)及整體存活期($P = 0.037$) 有顯著意義。參數 busyness 與 coarseness 變化與腫瘤體積變化呈現相關性($r = 0.835$ and $r = -0.368$)。

結論: 利用 PERCIST 標準評估轉移性肺腺癌接受得紓緩治療反應時，骨骼顯像上的復燃現象可能會影響判讀。此時，TLG-S 標準用於評估病患預後可能有較佳的幫助。對於影像紋理特性在疾病預後的解讀必須謹慎。

關鍵字: 肺癌；得紓緩；葡萄糖正子掃描；腫瘤反應；存活期；預後；紋理分析

英文摘要

Abstract

Purpose In this prospective study, we sought to investigate whether early FDG-PET assessment of treatment response using total lesion glycolysis measured with a systemic approach (TLG-S) could be superior to either local assessment with EORTC (European Organization for Research and Treatment of Cancer) criteria or single-lesion assessment with PERCIST (PET Response Criteria in Solid Tumors) for predicting clinical outcomes in patients with metastatic lung adenocarcinoma treated with erlotinib. The study hypothesis originated from the potential occurrence of the flare phenomenon and the differences in tumor biology between primary malignant cells and their metastasized progenies. In addition, the prognostic value of tumor textural features was investigated.

Methods We performed a retrospective review of prospectively collected data from 23 patients with metastatic lung adenocarcinoma treated with erlotinib. All participants underwent FDG-PET imaging at baseline and on days 14 and 56 after completion of erlotinib treatment. In addition, CT scans were performed at baseline and on day 56. FDG-PET response was assessed with TLG-S, EORTC, and PERCIST criteria. Response assessment based on RECIST 1.1 (Response Evaluation Criteria in Solid Tumors) from CT imaging was used as the reference standard. Regional textural features were analyzed using neighborhood grey-tone difference matrix with parameters of coarseness, contrast, busyness, complexity, and strength. Two-year progression-free survival (PFS) and overall survival (OS) served as the main outcome measures.

Results We identified 13 patients with bone metastases. Of them, four (31%) had bone flares at day 14 and were erroneously classified as non-responders according to the PERCIST criteria. Patients who were classified as responders on day 14 based on TLG-S criteria had higher 2-year PFS (26.7% vs. 0%, $P = 0.007$) and OS (40.0% vs. 7.7%, $P = 0.018$) rates. Similar rates were observed in patients who responded on day 56 according to the RECIST criteria based on CT imaging. Patients classified as responders on day 14 according to the EORTC criteria on FDG-PET imaging had a better 2-year OS rate compared with non-responders (36.4% vs. 8.3%, $P = 0.015$). The early change of busyness showed significantly better PFS ($P = 0.004$) and the coarseness change demonstrated significantly better outcomes in PFS ($P = 0.007$) and OS ($P = 0.037$). The busyness and coarseness changes were correlated with tumor volume changes ($r = 0.835$ and $r = -0.368$).
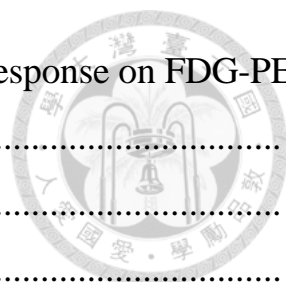
Conclusions Bone flares that can interfere with the interpretation of treatment response according to the PERCIST criteria are not uncommon in patients with metastatic lung adenocarcinoma treated with erlotinib. In this scenario, TLG-S criteria may help to better predict survival outcomes than other forms of assessment. Interpretation of textural features for prognosis should be cautious.

Keywords Lung cancer; erlotinib; FDG-PET; tumor response; survival; outcomes; textural analysis

目　錄

圖目錄

表目錄

論文正文

1. INTRODUCION

1.1 Erlotinib and gene mutation in lung cancer

Erlotinib (Tarceva®, Roche Products Ltd., Welwyn Garden City, UK) is a small-molecule inhibitor of the epidermal growth factor receptor (EGFR) tyrosine kinase enzymatic activity. Treatment with erlotinib is molecular targeted therapy for lung adenocarcinoma. Although patients carrying mutations of the *EGFR* gene generally respond better to tyrosine kinase inhibitors (TKIs) [1], erlotinib may improve survival even in subjects with *EGFR* wild-type tumors [2].

1.2 FDG-PET for erlotinib response assessment

Several studies have shown that FDG-PET is a useful imaging modality for predicting response to erlotinib in patients with non-small cell lung cancer (NSCLC) [3-19]. However, most of them utilized only the primary tumor as the target lesion for sequential imaging [3, 5, 6, 9, 10, 12-14, 17, 18]. Moreover, the European Organization for Research and Treatment of Cancer (EORTC) criteria [20] were mainly used to assess treatment response [3, 5, 9, 10, 12-14]. Conversely, other reports evaluated treatment response using the Positron Emission Tomography Response Criteria in Solid Tumors (PERCIST) [21] based on the measurement of standardized uptake value (SUV) − with a specific focus on the hottest single lesion [8, 11]. Finally, there have been studies that used the total lesion glycolysis measured with a systemic approach (TLG-S) based either on the sum of up to a maximum of five measurable target lesions [16] or all measurable lesions [19] .

1.3 Bone flares in FDG-PET response

In addition, bone flares in NSCLC patients treated with TKIs have been reported both in CT [22] and bone scan [23] studies. However, the effect of bone flares on FDG-PET in response evaluation has not been investigated.

1.4 The effect of tumor heterogeneity on drug response

Growing evidence indicates that significant differences in tumor biology exist between primary malignant cells and their metastasized progenies. In NSCLC, a significant discordance in *EGFR* and *K-RAS* mutation status has been reported between primary tumors and their corresponding lymph

1
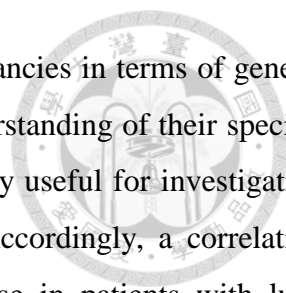
node metastases [24] or distant metastases [25, 26]. Owing to the discrepancies in terms of genetic alterations between primary and metastatic tumors [27-29], a deeper understanding of their specific metabolic phenotype on FDG-PET scans would be desirable and clinically useful for investigating the therapeutic response to TKIs in patients with advanced NSCLC. Accordingly, a correlation between *EGFR* mutation heterogeneity and a mixed FDG-PET response in patients with lung adenocarcinoma treated with TKIs has been reported [30]. Unfortunately, the question as to whether systemic assessments (i.e., including sites of distant metastases) of tumor response by FDG-PET would be superior to the exclusive focus on primary tumor response in this setting remains open.

1.5 Textural analysis for tumor heterogeneity

Intratumoral heterogeneity of FDG distribution in pre-treatment PET assessed by texture analysis may yield additional predictive and prognostic information [31]. Cook et al. reported abnormal texture features of primary tumor in baseline FDG-PET were associated with tumor response and survival outcomes in lung cancer patients [32]. Therefore, it is worthy to further investigate whether the temporal changes in the intratumoral heterogeneity might provide additional prognostic information about tumor response to erlotinib.

1.6 Study aims

Starting from these premises, we designed the current study to investigate whether early FDG-PET assessment of treatment response using TLG-S could be superior to either local assessment with EORTC criteria or single-lesion assessment with PERCIST for predicting clinical outcomes in patients with metastatic lung adenocarcinoma treated with erlotinib. The study hypothesis originated from the potential occurrence of the flare phenomenon and the differences in tumor biology between primary malignant cells and their metastasized progenies. In addition, the prognostic value of tumor textural features was investigated.

2. MATERIALS AND METHODS

2.1 Patients

Eligibility criteria for this study were as follows: 1) stage IIIB-IV lung adenocarcinoma or recurrent

2

adenocarcinoma of the lung that failed to respond to frontline chemotherapy or relapsed thereafter; 2) complete recovery from any toxic effects of previous antitumor therapy, and 3) no chemotherapy within one month of enrolment. Patients were excluded in presence of the following criteria: 1) symptomatic brain metastases; 2) severe comorbidities; 3) presence of malignant pleural effusion without other measurable lesions, and 4) active infections. The Institutional Review Board of the Chang Gung memorial hospital approved the study protocol. Written informed consent was obtained from all participants.

2.2 Study Design

This was a single-center, single-arm, open-label study. All patients received oral erlotinib at a fixed dose of 150 mg (one tablet per day). Baseline FDG-PET examinations (day 0 FDG-PET) were performed in the two weeks preceding the start of erlotinib therapy. Follow-up FDG-PET scans were performed at days 14 and 56 after the beginning of erlotinib for the assessment of early and late treatment response, respectively. CT scans were performed both at baseline and on day 56 (**Figure 1**).

Figure 1
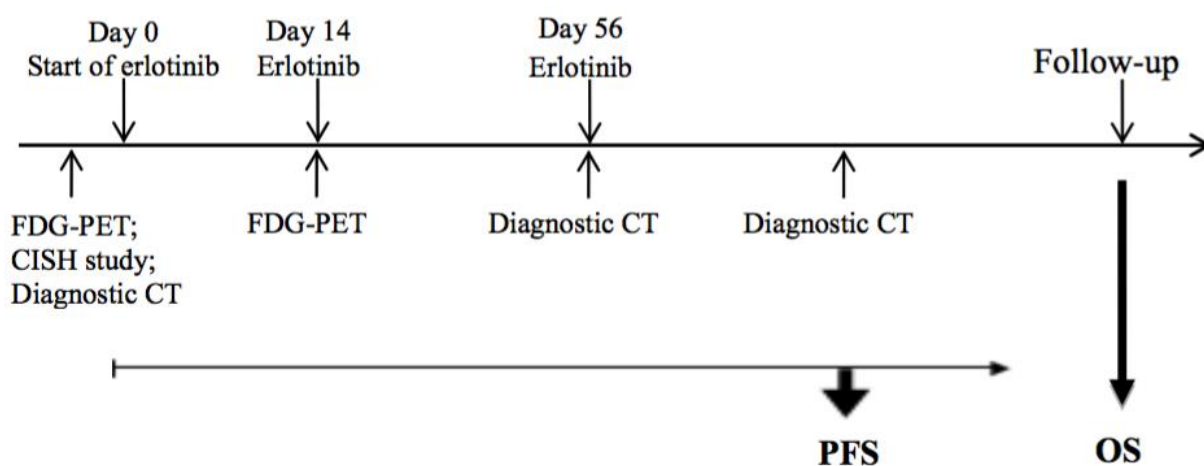
Study schema

2.3 FDG-PET/CT Image Acquisition

Patients were asked to fast 4 h before examination and blood glucose levels were <200 mg/dL in all participants. No intravenous contrast enhancement was used. Patients were injected intravenously with 370–555 MBq ^{18}F-FDG (depending on body weight) and images were acquired 50 min after its

3

administration. Whole-body PET emission scans were performed from the base of the skull to the mid-thigh with no position changes. FDG-PET/CT was performed using a Discovery ST 16 scanner (GE Healthcare, Milwaukee, WI, USA) in 18 patients, whereas the remaining 5 subjects were imaged on a Biograph mCT scanner (Siemens Medical Solutions, Malvern, PA, USA). Low-dose CT images were used for attenuation correction of PET data. PET images were reconstructed using a CT-based attenuation correction with an ordered-subset expectation maximization iterative reconstruction algorithm (4 iterations and 10 subsets for the Discovery ST16 scanner; 2 iterations and 21 subsets for the Biograph mCT scanner). Using these reconstruction parameters, axial spatial resolutions of PET at the center of the gantry were 4.80 mm and 2.16 mm for the Discovery ST16 and the Biograph mCT scanners, respectively. The two scanners were calibrated for quantitative correlation.

2.4 Imaging Analysis and Assessment of Treatment Response

2.4.1 PET parameters

FDG-PET images were obtained in transaxial planes using a dedicated workstation (Syngo; Siemens Medical Solutions). The SUV for each tumor volume was calculated with the following formula: (measured activity concentration [Bq/mL])/(injected activity [Bq]/body weight [kg] $\times$ 1,000). Rather than the peak SUV utilized by the PERCIST criteria, we measured the maximum SUV within a region of interest (ROI) [11]. A SUV >2.5 was used as the threshold for target volume delineation of the metabolic tumor volume (MTV) [33]. TLG-S was calculated as follows: TLG-S = mean SUV $\times$ MTV (cm^3) [34].

2.4.2 EORTC criteria

The metabolic response according to the EORTC criteria is based on the same ROI volumes sampled on subsequent scans. A partial metabolic response (PMR) was defined as a SUV reduction ≥25%. Stable metabolic disease (SMD) was diagnosed in presence of either an increase or a decrease <25%. Finally, progressive metabolic disease (PMD) was defined as a SUV increase >25% [20].

2.4.3 PERCIST criteria

In line with the standard procedures recommended by the PERCIST criteria, we measured the change in SUV between the hottest single tumor lesion on baseline scan and the hottest single lesion on the subsequent scan. The target lesions may differ between each scan. A complete

4

metabolic response (CMR) was defined as a complete abrogation of tumor FDG uptake; PMR as a SUV reduction of at least 30%; PMD as either a SUV increase of at least 30% or the development of a new lesion. Finally, SMD was considered to be present when CMR, PMR, and PMD did not occur [21].

2.4.4 TLG-S method

According to the PERCIST recommendations [21], the measurement of TLG-S was based on the delineation of target lesions (two lesions or less per organ, with a maximum of five lesions). PMR was defined as a reduction of at least 45% in TLG-S, whereas PMD was diagnosed in presence of a 75% or higher increase in this parameter [21]. SMD was considered to be present when PMR or PMD did not occur [21].

2.4.5 RECIST criteria

Standard CT response was assessed through an independent review of CT images obtained at day 56 compared with baseline scans. All CT images were analyzed by investigators blinded to PET results. Target lesions (two lesions or less per organ, with a maximum of five lesions) were identified. Tumor response was classified as complete response (CR), partial response (PR), stable disease (SD), or progressive disease (PD) according to the Response Evaluation Criteria in Solid Tumors (RECIST), version 1.1 [35]. Based on FDG-PET results, patients with CMR or PMR were considered as responders whereas those with SMD or PMD were classified as non-responders. Patients with CR or PR on CT images were classified as responders, whereas those who showed SD or PD were considered as non-responders.

2.5 Texture analysis

Distinct sets of texture features can be extracted from PET images using different matrices. In the present study, we used neighborhood grey-tone difference matrix (NGTDM) for the assessment of third-order texture features [31]. The texture parameters of coarseness, contrast, busyness, complexity, and strength were calculated from the NGTDM according to previous literatures of lung cancer studies [32, 36]. The computations of the textural features were performed using a homemade software package (Chang-Gung Image Texture Analysis toolbox; CGITA) implemented under MATLAB 2012a (Mathworks Inc., Natick, MA, USA) [37].

5
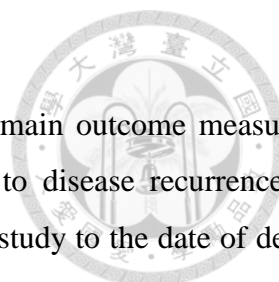
2.6 Statistical Analysis

Progression-free survival (PFS) and overall survival (OS) served as the main outcome measures. PFS was defined as the time from the date of inclusion in the study to disease recurrence or progression. OS was defined as the time from the date of inclusion in the study to the date of death from any cause or last follow-up. Survival curves were plotted with the Kaplan-Meier method and compared using the log-rank test. Cox regression analysis was used to calculate the adjusted hazard ratios (HRs) and their corresponding 95% confidence intervals (CIs). All calculations were performed with the SPSS 18.0 statistical package (SPSS Inc. Chicago, IL, USA). Two-tailed P values < 0.05 were considered statistically significant.

3. RESULTS

3.1 Patients

Between April 2009 and May 2012, we identified a total of 23 patients (16 women and 7 men) with advanced lung adenocarcinoma who were treated with erlotinib (**Table 1**).

3.2 Response on FDG-PET *versus* CT imaging according to the RECIST criteria

All patients underwent FDG-PET imaging at day 14, whereas data for day 56 FDG-PET scans were missing for three participants.

Based on FDG-PET imaging at day 14 and according to the EORTC criteria, there were 11 patients (48%) who had PMR, 11 (48%) with SMD, and 1 (4%) with PMD. According to FDG-PET imaging at day 56, we identified 5 patients (25%) with CMR, 7 (35%) with PMR, 5 (25%) with SMD, and 3 (15%) with PMD.

Based on FDG-PET imaging at day 14 and according to the PERCIST criteria, there were 6 patients (26%) who had PMR, 15 (65%) with SMD, and 2 patients (9%) with PMD. According to FDG-PET imaging at day 56, we identified 1 patient (5%) with CMR, 8 patients (40%) with PMR, 7 patients (35%) with SMD, and 4 patients (20%) with PMD.

Based on FDG-PET imaging at day 14 and according to the TLG-S criteria (summing up the five hottest lesions), there were 10 patients (26%) who had PMR, 11 patients (65%) with SMD, and 2 patients (9%) with PMD. According to FDG-PET imaging at day 56, we identified 1 patient (5%)
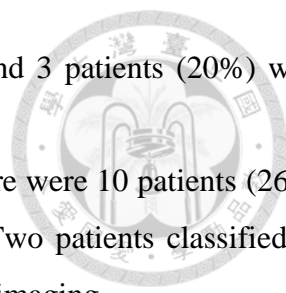
with CMR, 8 patients (40%) with PMR, 8 patients (35%) with SMD, and 3 patients (20%) with PMD.

Based on CT imaging at day 56 and according to the RECIST criteria, there were 10 patients (26%) who had PR, 5 patients (65%) with SD, and 8 patients (9%) with PD. Two patients classified as having PD and one patient who had PR did not undergo day 56 FDG-PET imaging.

The overall response according to early FDG-PET findings *versus* the standard CT response is summarized in **Table 2**.

Four patients who were classified as responders based on CT imaging at day 56 and according to the RECIST criteria were considered as non-responders when the PERCIST criteria were applied on early FDG-PET findings (**Figure 2**).

The median age at enrollment was 57 years. Most of the study patients (87%) had an ECOG performance status 0 or 1. The median follow-up time in the study cohort was 14 months (range, 1–51 months). At the end of the follow-up period, two patients survived and 21 died. The two patients who survived had a follow-up time of 51 and 39 months, respectively.

The overall response rate (43.5%, 10 out of 23 patients) obtained when the TLG-S system was applied to early FDG-PET results was identical to the overall response rate calculated by applying the RECIST criteria to CT data obtained on day 56. Eight patients with PD according to the RECIST criteria on day 56 were all classified as non-responders when the PERCIST and TLG-S criteria were applied on early FDG-PET findings; however, one of these subjects was classified as a responder based on the EORTC criteria. Taking into account that three patients had missing FDG-PET results, tumor response based on the PERCIST and TLG-S criteria using day 56 FDG-PET data (9 responders and 11 non-responders) was the same as that observed when the RECIST criteria were applied to CT findings (10 responders and 13 non-responders).

7

Table 1
General characteristics of the study patients [38]

Characteristic	Patients, *n* (%)
Number of patients	23 (100)
Age (years)	
Median	57
Range	38−81
Sex	
Male	7 (30)
Female	16 (70)
Performance status	
0	7 (30)
1	13 (57)
2	3 (13)
AJCC clinical stage[a]	
IIIB	1 (4)
IV	17 (74)
Post-operative recurrence	5 (22)

[a] Seventh edition.
AJCC American Joint Committee on Cancer.

Table 2
Overall response according to early FDG-PET findings *versus* standard CT response [38]

		Day 56 RECIST criteria	
		Responder	Non-responder
Day 14 EORTC criteria	Responder	9	2
	Non-responder	1	11
Day 14 PERCIST criteria	Responder	6	0
	Non-responder	4	13
Day 14 TLG-S criteria	Responder	10	0
	Non-responder	0	13

RECIST Response Evaluation Criteria in Solid Tumors version 1.1, *EORTC* European Organization for Research and Treatment of Cancer, *PERCIST* PET Response Criteria in Solid Tumors, *TLG-S* Total Lesion Glycolysis-Systemic approach.

Figure 2
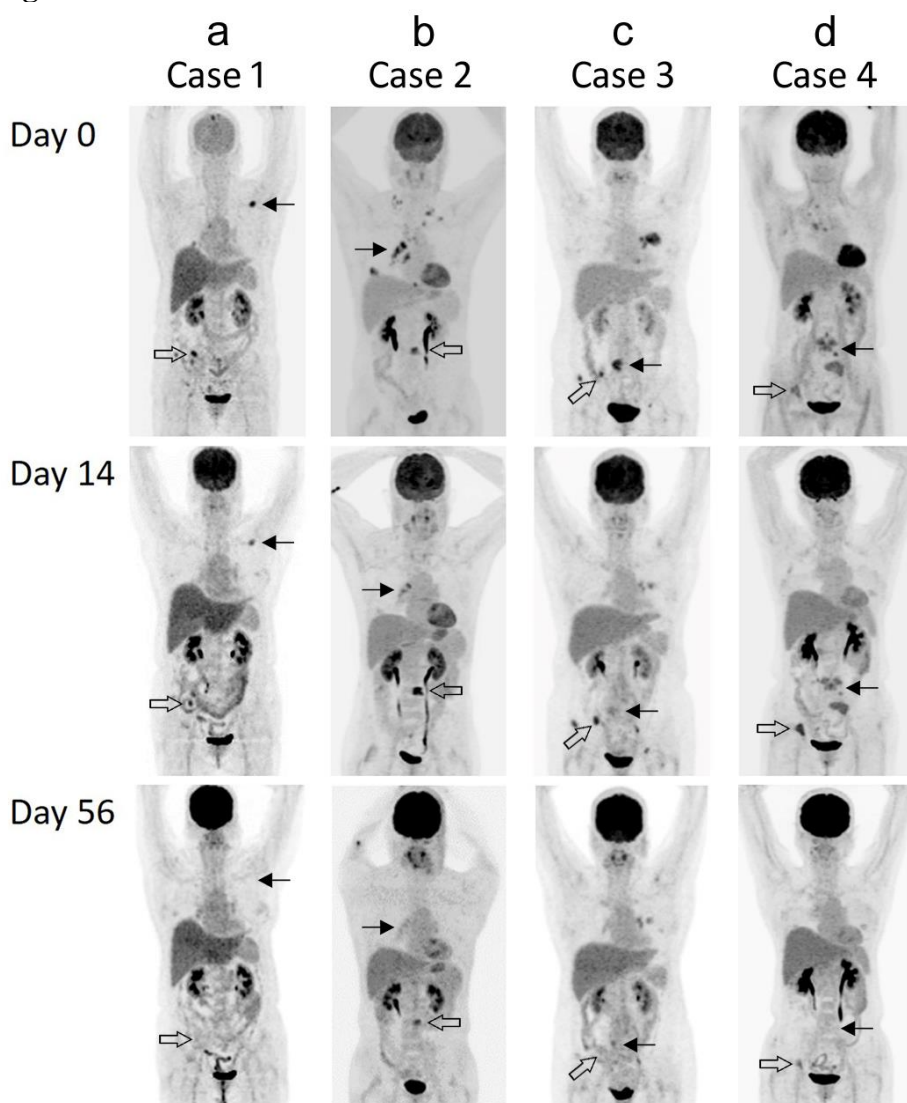
Illustrative images of four non-responders by PERCIST criteria on day 14 PET who had persistent bone uptake due to the bone flare effect during erlotinib treatment (case No. in **Figure 2** corresponded to the case No. in **Table 3**). (**a**) In case 1, the hottest lesion was identified at the scapula ($SUV_{max}$ 8.1; arrow) on day 0. On day 14, the hottest lesion was located at the ilium (SUV_{max} 7.3; hollow arrow). A complete metabolic response was observed on day 56. (**b**) In case 2, the hottest lesion was identified at mediastinal lymph nodes (SUV_{max} 15.3; arrow) on day 0. On day 14, the hottest lesion was located at the L3 spine (SUV_{max} 11.5; hollow arrow). On day 56, a partial metabolic response was observed, with tracer uptake being decreased at the L3 spine (SUV_{max} 5.3; hollow arrow). (**c**) In case 3, the hottest lesion was identified at the L5 spine (SUV_{max} 10.3; arrow) on day 0. On day 14, the hottest lesion was located at the sacroiliac junction (SUV_{max} 8.2; hollow arrow). On day 56, a decreased activity at the L5 spine (SUV_{max} 3.2) was observed (arrow) and the lesion located at the sacroiliac junction was not measurable (hollow arrow). (**d**) In case 4, the hottest lesion was identified at the lumbosacral spine (SUV_{max} 6.6; arrow) on day 0. On day 14, the hottest lesion was located at the acetabulum (SUV_{max} 6.2; hollow arrow). On day 56, a partial metabolic response was observed, with tracer uptake being decreased at the acetabulum (SUV_{max} 3.5; hollow arrow) [38].
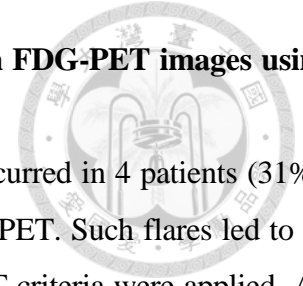
3.3 Impact of bone flares on early assessment of treatment response on FDG-PET images using the PERCIST criteria

A total of 13 study patients had bone metastases (**Table 3**). Bone flares occurred in 4 patients (31%), with the highest tracer uptake in the bone being identified on day 14 FDG-PET. Such flares led to an erroneous classification of these patients as non-responders when PERCIST criteria were applied. All of the bone flares regressed on day 56 FDG-PET images (**Figure 2**). Notably, all of these four patients were correctly classified as responders according to either the EORTC or TLG-S criteria on day 14 (**Figure 3**).

All of the four patients identified as non-responders on day 14 according to the PERCIST criteria were classified as responders based on day 56 CT findings (Group A in **Table 3**). Of the remaining nine patients who did not have bone flares, 3 patients were classified as responders (Group B) and 6 as non-responders (Group C) according to the PERCIST criteria applied to day 14 FDG-PET results and RECIST approach applied to day 56 CT findings (**Table 3**).

Table 3

Changes of FDG uptake observed in bone lesions and in the hottest single lesions identified during erlotinib treatment among patients with lung cancer and skeletal metastases [38]

| Group	Case no.	Day 0 (SUV)	Day 14 (SUV)	Day 56 (SUV)
A[a]	1	Bone (8.1)[b]	Bone (7.3)[b]	Bone (−)
Day 14 PERCIST criteria: non-responders	2	Bone (11.3), MLN (15.3)[b]	Bone (11.5)[b]	Bone (5.3)[b]
Day 56 RECIST criteria: responders	3	Bone (10.3)[b]	Bone (8.2)[b]	Bone (3.2), MLN (5.0)[b]
	4	Bone (6.6)[b]	Bone (6.2)[b]	Bone (3.5)[b]
B	5	Bone (21.8)[b]	Bone (8.2)[b]	Bone (2.8), MLN (5.3)[b]
Day 14 PERCIST criteria: responders	6	Bone (9.2)[b]	Bone (5.3)[b]	Bone (3.6)[b]
Day 56 RECIST criteria: responders	7	Bone (6.6), liver (7.7)[b]	Bone (4.2), MLN (4.9)[b]	Bone (−), MLN (4.2)[b]
C	8	Bone (5.6), lung (7.1)[b]	Bone (8.8)[b]	Bone (11.9)[b]
Day 14 PERCIST criteria: non-responders	9	Bone (6.8)[b]	Bone (7.8)[b]	Bone (3.9), lung (6.1)[b]
Day 56 RECIST criteria: non-responders	10	Bone (9.4)[b]	Bone (9.0)[b]	Bone (6.8)[b]
	11	Bone (13.0)[b]	Bone (9.6)[b]	Bone (9.3)[b]
	12	Bone (8.4), lung (10.5)[b]	Bone (7.4), lung (11.3)[b]	N/A
	13	Bone (8.0), lung (13.4)[b]	Bone (8.8), lung (15.5)[b]	Bone (8.3), lung (16.4)[b]

PERCIST PET Response Criteria in Solid Tumors, *RECIST* Response Evaluation Criteria in Solid Tumors version 1.1, *MLN* mediastinal lymph node, *N/A* not available

[a] Group A was the bone flare group

[b] Hottest lesion identified during a whole-body PET scan

Figure 3
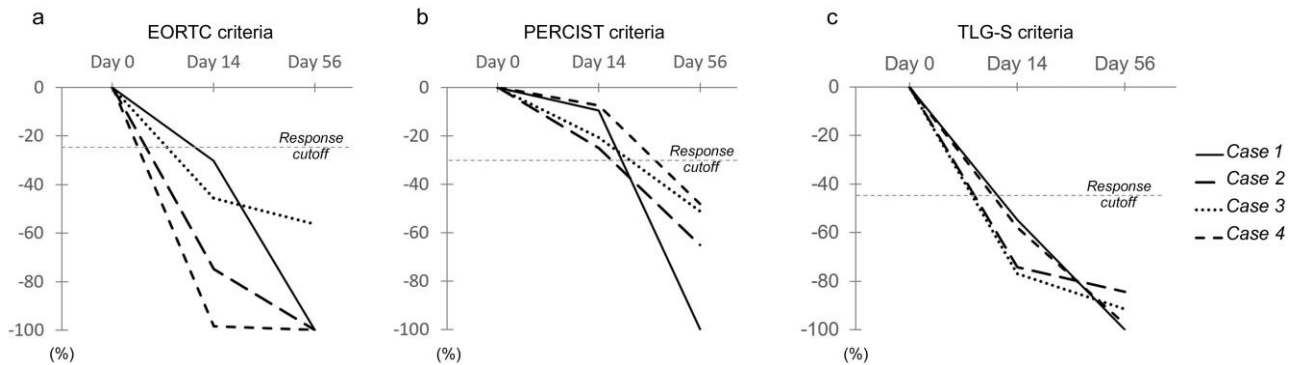
Percentage changes of FDG uptake in the four patients with skeletal metastases who were erroneously classified as non-responders according to FDG-PET imaging at day 14 using the PERCIST criteria (**a**). All of these patients were correctly classified as early responders according to the EORTC criteria (**b**). The use of a systemic approach that included both primary and metastatic tumors (TLG-S method) was similarly effective in classifying these patients as early responders (**c**). The cut-off values for defining a reduction of FDG uptake as significant were 25%, 30%, and 45% of baseline values for EORTC, PERCIST, and TLG-S criteria, respectively [38].

3.4 Prediction of progression-free survival

Patients who were classified as responders on day 14 based on TLG-S criteria had higher 2-year PFS (26.7% *vs*. 0%; $P = 0.007$ [log-rank test, Kaplan-Meier analysis], **Figure 4**; HR = 0.28, 95% CI = 0.10−0.76, $P = 0.012$). However, the assessment of early response on FDG-PET scans based on either EORTC or PERCIST criteria was not significantly associated with PFS. Using FDG-PET images obtained at day 56, we identified significant univariate associations between 2-year PFS and response according to both PERCIST (16.7% *vs*. 0%; $P = 0.044$ [log-rank test, Kaplan-Meier analysis]; HR = 0.37, 95% CI = 0.13−1.03, $P = 0.057$) and TLG-S PERCIST (16.7% *vs*. 0%; $P = 0.044$ [log-rank test, Kaplan-Meier analysis]; HR = 0.37, 95% CI = 0.13−1.03, $P = 0.057$) criteria. On day 56, CT response according to the RECIST was significantly associated with a higher 2-year PFS rate (26.7% *vs*. 0%; $P = 0.007$ [log-rank test, Kaplan-Meier analysis]; HR = 0.28, 95% CI = 0.10−0.76, $P = 0.012$). However, FDG-PET response according to the EORTC criteria did not show a statistically significant association with PFS.

3.5 Prediction of overall survival

Patients who were classified as responders on day 14 based on the EORTC criteria had higher 2-year OS (36.4% *vs*. 8.3%; $P = 0.015$ [log-rank test, Kaplan-Meier analysis]; HR = 0.32, 95% CI = 0.12−0.83, $P = 0.020$). Similar findings were obtained when responders were identified with the

TLG-S method (40.0% *vs*. 7.7%; $P = 0.018$ [log-rank test, Kaplan-Meier analysis], **Figure 5**; HR = 0.32, 95% CI = 0.12−0.86, $P = 0.024$). Early FDG-PET response according to the PERCIST criteria was not significantly associated with OS. On day 56, CT response based on the RECIST criteria was the only variable significantly associated with 2-year OS (40.0% *vs*. 7.7%; $P = 0.018$ [log-rank test, Kaplan-Meier analysis], **Figure 5**; HR = 0.32, 95% CI = 0.12−0.86, $P = 0.024$). Although patients classified as responders or non-responders according to PERCIST and TLG-S on day 56 were the same as those identified using the RECIST criteria, the association between FDG-PET response and OS was not significant because of missing data in three participants.

Figure 4
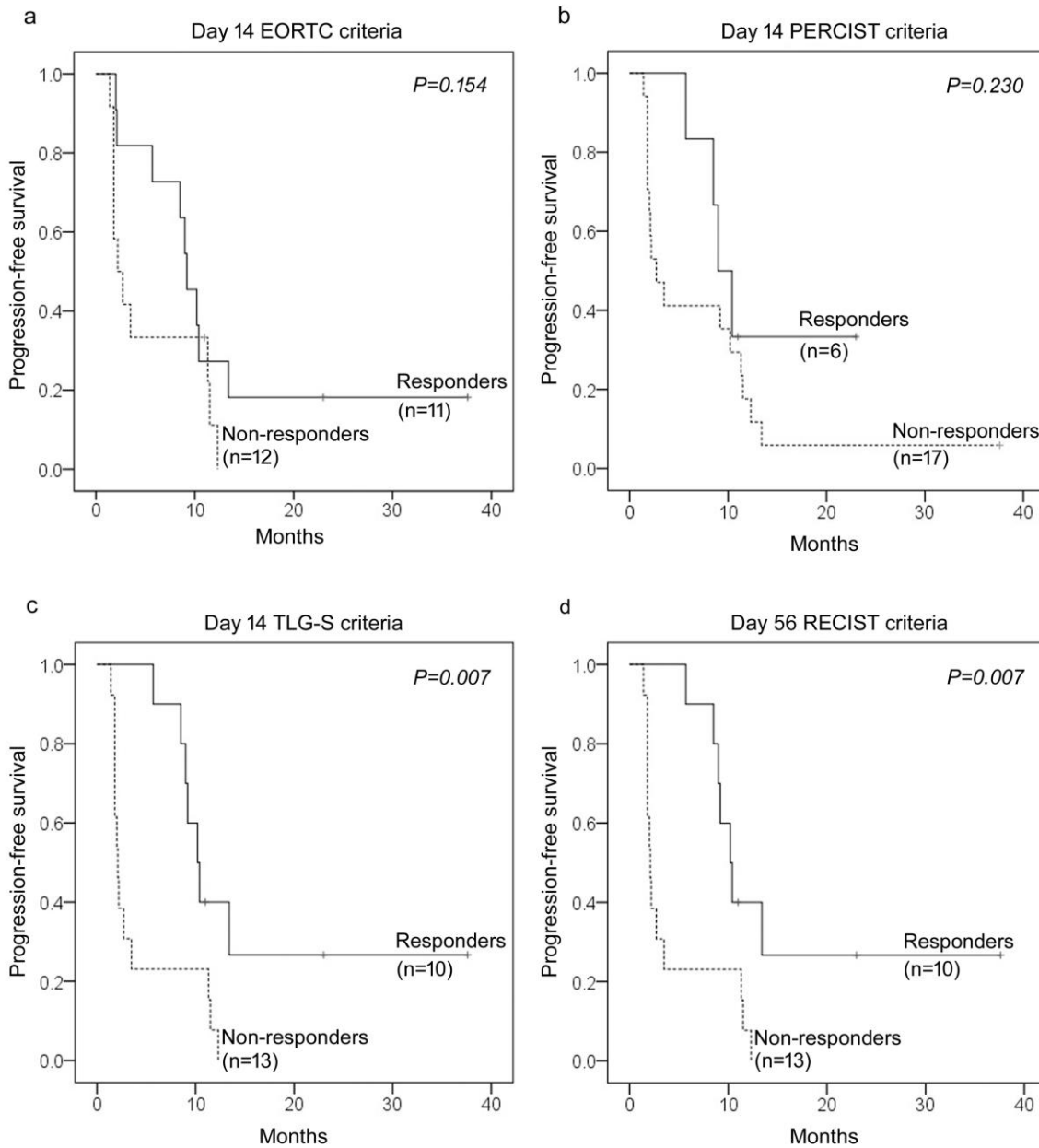
Kaplan-Meier estimates of progression-free survival (PFS) according to different criteria used for assessing FDG-PET response. No significant differences in terms of PFS were identified between responders and non-responders defined according to FDG-PET imaging at day 14 using either the EORTC criteria (**a**) or the PERCIST criteria (**b**). Patients classified as responders according to FDG-PET imaging at day 14 using the TLG-S criteria (**c**) and according to CT imaging at day 56 using the RECIST criteria (**d**) had an identically higher PFS ($P = 0.007$) [38].
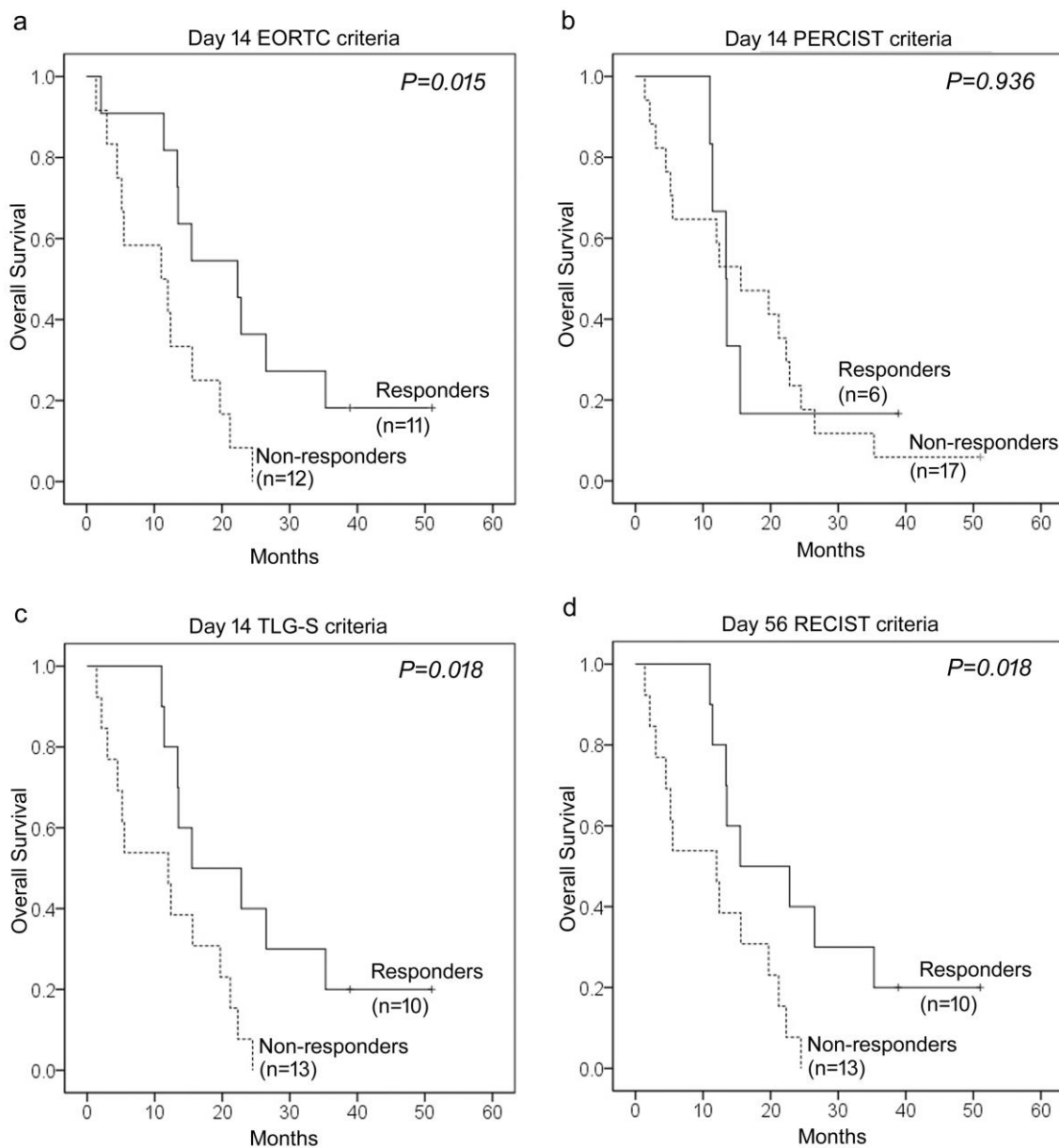
Figure 5

Kaplan-Meier estimates of overall survival (OS) according to different criteria used for assessing FDG-PET response. Patients classified as responders according to FDG-PET imaging at day 14 using the EORTC criteria had a significantly better OS ($P = 0.015$) (**a**). No significant differences in terms of OS were identified between responders and non-responders defined according to FDG-PET imaging at day 14 using the PERCIST criteria (**b**). Patients classified as responders according to FDG-PET imaging at day 14 using the TLG-S criteria (**c**) and according to CT imaging at day 56 using the RECIST criteria (**d**) had an identically higher OS ($P = 0.018$) [38].

3.6 Textural parameters for survival prediction

By ROC curves for tumor textural features, the cut-off values of parameters derived from NGTDM such as coarseness, busyness, contrast, and complexity for pre-treatment baseline and early change

during treatment were identified. No significant pre-treatment parameters were identified for outcome prediction in PFS and OS. For early change on day 14, the busyness with decrease >32% showed significantly better PFS (P = 0.004) and marginal better OS (P = 0.089). The coarseness with increase >64% demonstrated significantly better outcomes in PFS (P = 0.007) and OS (P = 0.037). However, the change of busyness value was strongly correlated with tumor volume change (r = 0.835, P < 0.001) and the change of coarseness value was moderately correlated with tumor volume change (r = -0.368, P = 0.084).

4. DISCUSSION

4.1 Why the results of PERCIST criteria is inconsistent with other groups?
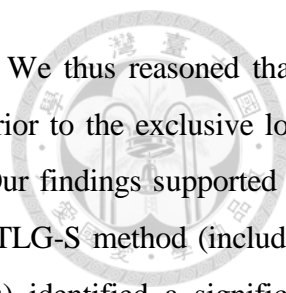
The PERCIST criteria utilize the hottest lesion on FDG-PET as target, considering both the primary tumor and its distant metastases. In a study conducted in 22 patients, Benz *et al.* [11] reported that patients who had PMD according to FDG-PET results obtained at two weeks after the start of erlotinib treatment displayed a significantly shorter time to progression and a poorer OS compared with those showing either SMD or PMR. Another report by Zander *et al.* [8] demonstrated that the PERCIST criteria obtained using FDG-PET data acquired after one week of erlotinib therapy predicted both PFS and OS in patients with advanced NSCLC independent of the *EGFR* mutation status. Similar results were obtained when the EORTC criteria were applied [8]. However, the results of our study indicate that FDG-PET response according to the PERCIST criteria on day 14 was not significantly associated with PFS and OS. A potential explanation for these findings is that some patients classified as responders according to CT imaging at day 56 using the RECIST criteria were erroneously considered as non-responders based on early FDG-PET results. Notably, incorrect patient classification was mainly caused by a high skeletal tracer uptake on day 14, ultimately resulting in a markedly lower SUV reduction compared with other study participants. It should be indeed noted that 1) all of these bone lesions disappeared on day 56 and 2) the four patients incorrectly classified by the PERCIST criteria were correctly identified as early responders according to both the EORTC and TLG-S criteria. Starting from these premises, bone flares are a plausible explanation for misclassification when PERCIST criteria are used.

4.2 The effects of bone flare

In this study, we observed that the presence of "persistent bone uptake" in patients who showed primary tumor response resulted in an erroneous categorization of four patients (group A in **Table 3**). Although the discrepancy between primary tumor (response) and bone metastasis (no-response) on day 14 may be caused by tumor heterogeneity, bone uptake was either much decreased or absent on day 56 in group A patients. Based on these findings, we reasoned that the occurrence of bone flares would be the most plausible mechanism to explain "discordant persistent" tracer uptake in the bone. However, the peak time of bone flare can be influenced by several factors (e.g., tracer, tumor type, and drugs). Numerous data on bone flares are available from bone scintigraphy studies but less information is available on their occurrence in FDG-PET images. In this study, we defined persistent bone uptake as a SUV_{max} reduction of less than 30% or an increase in SUV_{max} values. Persistent bone uptake observed on day 14 imaging may have occurred before or after peak time. Consequently, non-peak persistent bone uptake was attributed to the bone flare phenomenon. The clinical significance of the bone flare phenomenon is still a matter of debate [39]. Osteoblastic bone flares have been previously described as transiently worsening bone lesions on FDG-PET scans in a case series of four NSCLC patients treated with bevacizumab [40]. Another study using CT imaging and the RECIST criteria identified the occurrence of osteoblastic bone flares in three NSCLC patients who received erlotinib [22]. It has been reported that 21% of NSCLC patients who undergo bone scintigraphy develop bone flares during therapy with TKIs [23]. In the present study, bone flares were observed in 31% of patients with skeletal metastases on FDG-PET scans performed on day 14. Nonetheless, a case report that used FDG-PET for the assessment of response to erlotinib indicated that disease progression might be misdiagnosed as a bone flare as well [41]. In our study, six non-responders with persistent bone lesions on day 14 had stable disease on day 56.

4.3 Tumor heterogeneity: systemic approach *vs*. local assessment

Consistent with previous reports [3, 5, 9, 10, 12-14], the results of our study demonstrate that assessment of early FDG-PET response using the EORTC criteria predicts OS in NSCLC patients treated with erlotinib. In our report, the number and timing of FDG-PET scans (at baseline and on days 14 and 56) were in line with the protocol utilized by Mileshkin *et al.* [9]. Interestingly, these authors reported that FDG-PET response according to the EORTC criteria on day 14 was significantly associated with a better OS, whereas the same response on day 56 was not. Nonetheless, the biological heterogeneity between the primary tumor and its metastatic progenies as well as the intermetastatic

heterogeneity [42] have not been previously taken into adequate account. We thus reasoned that a systemic assessment that would include the metastatic sites could be superior to the exclusive local assessment of primary tumor response according to the EORTC criteria. Our findings supported the original study hypothesis. Accordingly, a systemic approach based on the TLG-S method (including both primary and metastatic tumors up to a total of five target lesions) identified a significant association between early FDG-PET response and survival endpoints (PFS and OS).

4.4 Proposed TLG-S method

In line with the PERCIST criteria, in this study we defined PMR as a reduction of at least 45% in TLG-S, whereas PMD was diagnosed in presence of a 75% or higher increase in this parameter. Kahraman *et al.* [16] have previously shown that the percentage change of TLG-S is a strong predictor of survival outcomes in NSCLC patients treated with erlotinib. In their study, the authors defined TLG-S as the sum of up to a maximum of five measurable target lesions; different cut-off values for defining the metabolic response were also calculated [16]. Another recent report demonstrated that high TLG-S values are an independent predictor of survival in patients with advanced NSCLC who receive erlotinib [19]. In the latter study, TLG-S was calculated by taking into account all of the measurable lesions in whole-body scans; in addition, TLG-S was dichotomized according to the median value [19]. Altogether these findings indicate a strong prognostic significance of TLG-S, although both the extent of target lesions and the definition of metabolic response have not yet been standardized.

4.5 Impact of tumor heterogeneity

Some controversy still exists on the discordance in *EGFR* and *K-RAS* mutation status between primary and metastatic tumors among NSCLC patients [24-26]. Therefore, local imaging assessment of the primary tumor has been mainly supported by reports showing that a heterogeneous distribution of *EGFR* mutations occurs rarely [43, 44]. In our study, we demonstrate that FDG-PET response based on the EORTC criteria is associated with OS but not PFS. However, it should be noted that small core biopsies may not correctly reflect the clonal heterogeneity of the entire tumor [45]. Moreover, intratumor heterogeneity (consisting of a mixed population of *EGFR*-mutated and wild-type cells) may reduce the response to TKIs [46]. A significant heterogeneity in the *EGFR* mutation status between primary lung tumors and their metastases can also cause a mixed response to TKIs in certain patients [30, 45]. At the imaging level, the intratumor heterogeneity of FDG uptake has been associated with

tumor response and clinical outcomes in NSCLC patients treated with erlotinib [18]. Based on these findings, we believe that systemic approaches including distant metastases would be superior to single-site assessments when this patient group undergoes FDG-PET imaging. Our current findings obtained with the TLG-S method supports this contention quite strongly.
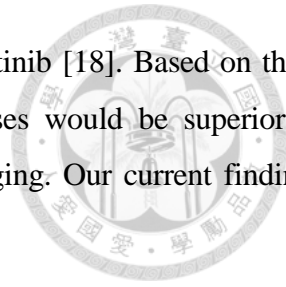
4.6 Limitation of textural analysis in current study

We found the high correlation between textural parameters and tumor volume. Therefore, it should be cautious when interpreting the usefulness of texture features for tumor prognosis [47]. Besides, it has been shown that the sensitivity of PET textural features to normal stochastic image variation and imaging parameters can be significant [48]. With very limited number of patients being included, stochastic variability of PET textural parameters might therefore have greatly confounded the results of the study. Further study with more patients included should be conducted to verify the role of textural features in tumor response evaluation and prognosis prediction.

5. CONCLUSIONS

The results of the present study demonstrate that TLG-S criteria may help to better predict PFS and OS than other forms of assessment based on early FDG-PET response. Bone flares that can interfere with the interpretation of treatment response according to the PERCIST criteria are not uncommon in patients with metastatic lung adenocarcinoma treated with erlotinib. The high correlation between textural parameters and tumor volume limited the value of prognostic evaluation.
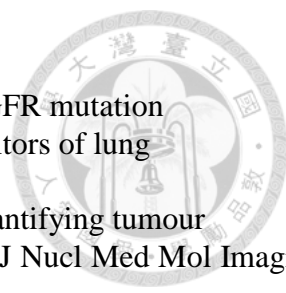
參考文獻

1. Lynch TJ, Bell DW, Sordella R, Gurubhagavatula S, Okimoto RA, Brannigan BW, et al. Activating mutations in the epidermal growth factor receptor underlying responsiveness of non-small-cell lung cancer to gefitinib. The New England journal of medicine. 2004;350:2129-39.
2. Cappuzzo F, Ciuleanu T, Stelmakh L, Cicenas S, Szczesna A, Juhasz E, et al. Erlotinib as maintenance treatment in advanced non-small-cell lung cancer: a multicentre, randomised, placebo-controlled phase 3 study. The Lancet Oncology. 2010;11:521-9.
3. van Gool MH, Aukema TS, Schaake EE, Rijna H, Valdes Olmos RA, van Pel R, et al. Timing of metabolic response monitoring during erlotinib treatment in non-small cell lung cancer. J Nucl Med. 2014;55:1081-6.
4. Hachemi M, Couturier O, Vervueren L, Fosse P, Lacoeuille F, Urban T, et al. [(1)(8)F]FDG positron emission tomography within two weeks of starting erlotinib therapy can predict response in non-small cell lung cancer patients. PloS one. 2014;9:e87629.
5. Schaake EE, Kappers I, Codrington HE, Valdes Olmos RA, Teertstra HJ, van Pel R, et al. Tumor response and toxicity of neoadjuvant erlotinib in patients with early-stage non-small-cell lung cancer. J Clin Oncol. 2012;30:2731-8.
6. Kobe C, Scheffler M, Holstein A, Zander T, Nogova L, Lammertsma AA, et al. Predictive value of early and late residual 18F-fluorodeoxyglucose and 18F-fluorothymidine uptake using different SUV measurements in patients with non-small-cell lung cancer treated with erlotinib. Eur J Nucl Med Mol Imaging. 2012;39:1117-27.
7. Bengtsson T, Hicks RJ, Peterson A, Port RE. 18F-FDG PET as a surrogate biomarker in non-small cell lung cancer treated with erlotinib: newly identified lesions are more informative than standardized uptake value. J Nucl Med. 2012;53:530-7.
8. Zander T, Scheffler M, Nogova L, Kobe C, Engel-Riedel W, Hellmich M, et al. Early prediction of nonprogression in advanced non-small-cell lung cancer treated with erlotinib by using [(18)F]fluorodeoxyglucose and [(18)F]fluorothymidine positron emission tomography. J Clin Oncol. 2011;29:1701-8.
9. Mileshkin L, Hicks RJ, Hughes BG, Mitchell PL, Charu V, Gitlitz BJ, et al. Changes in 18F-Fluorodeoxyglucose and 18F-Fluorodeoxythymidine Positron Emission Tomography Imaging in Patients with Non-Small Cell Lung Cancer Treated with Erlotinib. Clinical cancer research : an official journal of the American Association for Cancer Research. 2011;17:3304-15.
10. Binns DS, Pirzkall A, Yu W, Callahan J, Mileshkin L, Conti P, et al. Compliance with PET acquisition protocols for therapeutic monitoring of erlotinib therapy in an international trial for patients with non-small cell lung cancer. Eur J Nucl Med Mol Imaging. 2011;38:642-50.
11. Benz MR, Herrmann K, Walter F, Garon EB, Reckamp KL, Figlin R, et al. (18)F-FDG PET/CT for monitoring treatment responses to the epidermal growth factor receptor inhibitor erlotinib. J Nucl Med. 2011;52:1684-9.
12. Aukema TS, Kappers I, Olmos RA, Codrington HE, van Tinteren H, van Pel R, et al. Is 18F-FDG PET/CT useful for the early prediction of histopathologic response to neoadjuvant erlotinib in patients with non-small cell lung cancer? J Nucl Med. 2010;51:1344-8.
13. van Gool MH, Aukema TS, Schaake EE, Rijna H, Codrington HE, Valdes Olmos RA, et al. (18)F-fluorodeoxyglucose positron emission tomography versus computed tomography in predicting histopathological response to epidermal growth factor receptor-tyrosine kinase inhibitor treatment in resectable non-small cell lung cancer. Annals of surgical oncology.
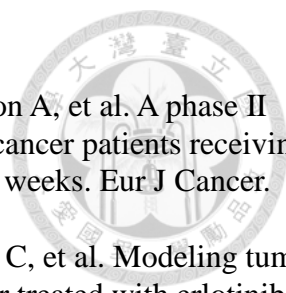
2014;21:2831-7.

14. O'Brien ME, Myerson JS, Coward JI, Puglisi M, Trani L, Wotherspoon A, et al. A phase II study of (1)(8)F-fluorodeoxyglucose PET-CT in non-small cell lung cancer patients receiving erlotinib (Tarceva); objective and symptomatic responses at 6 and 12 weeks. Eur J Cancer. 2012;48:68-74.

15. Suleiman AA, Frechen S, Scheffler M, Zander T, Kahraman D, Kobe C, et al. Modeling tumor dynamics and overall survival in advanced non-small-cell lung cancer treated with erlotinib. J Thorac Oncol. 2015;10:84-92.

16. Kahraman D, Holstein A, Scheffler M, Zander T, Nogova L, Lammertsma AA, et al. Tumor lesion glycolysis and tumor lesion proliferation for response prediction and prognostic differentiation in patients with advanced non-small cell lung cancer treated with erlotinib. Clin Nucl Med. 2012;37:1058-64.

17. de Langen AJ, van den Boogaart V, Lubberink M, Backes WH, Marcus JT, van Tinteren H, et al. Monitoring response to antiangiogenic therapy in non-small cell lung cancer using imaging markers derived from PET and dynamic contrast-enhanced MRI. J Nucl Med. 2011;52:48-55.

18. Cook GJ, O'Brien ME, Siddique M, Chicklore S, Loi HY, Sharma B, et al. Non-Small Cell Lung Cancer Treated with Erlotinib: Heterogeneity of F-FDG Uptake at PET-Association with Treatment Response and Prognosis. Radiology. 2015;0:141309.

19. Winther-Larsen A, Fledelius J, Sorensen BS, Meldgaard P. Metabolic tumor burden as marker of outcome in advanced EGFR wild-type NSCLC patients treated with erlotinib. Lung Cancer. 2016;94:81-7.

20. Young H, Baum R, Cremerius U, Herholz K, Hoekstra O, Lammertsma AA, et al. Measurement of clinical and subclinical tumour response using [18F]-fluorodeoxyglucose and positron emission tomography: review and 1999 EORTC recommendations. European Journal of Cancer. 1999;35:1773-82.

21. Wahl RL, Jacene H, Kasamon Y, Lodge MA. From RECIST to PERCIST: Evolving Considerations for PET Response Criteria in Solid Tumors. Journal of Nuclear Medicine. 2009;50:122S-50S.

22. Lind JSW, Postmus PE, Smit EF. Osteoblastic Bone Lesions Developing During Treatment with Erlotinib Indicate Major Response in Patients with Non-small Cell Lung Cancer: A Brief Report. Journal of Thoracic Oncology. 2010;5:554-7.

23. Chao HS, Chang CP, Chiu CH, Chu LS, Chen YM, Tsai CM. Bone scan flare phenomenon in non-small-cell lung cancer patients treated with gefitinib. Clin Nucl Med. 2009;34:346-9.

24. Schmid K, Oehl N, Wrba F, Pirker R, Pirker C, Filipits M. EGFR/KRAS/BRAF mutations in primary lung adenocarcinomas and corresponding locoregional lymph node metastases. Clinical cancer research : an official journal of the American Association for Cancer Research. 2009;15:4554-60.

25. Kalikaki A, Koutsopoulos A, Trypaki M, Souglakos J, Stathopoulos E, Georgoulias V, et al. Comparison of EGFR and K-RAS gene status between primary tumours and corresponding metastases in NSCLC. British journal of cancer. 2008;99:923-9.

26. Takahashi K, Kohno T, Matsumoto S, Nakanishi Y, Arai Y, Yamamoto S, et al. Clonal and Parallel Evolution of Primary Lung Cancers and Their Metastases Revealed by Molecular Dissection of Cancer Cells. Clinical Cancer Research. 2007;13:111-20.

27. Marusyk A, Almendro V, Polyak K. Intra-tumour heterogeneity: a looking glass for cancer? Nat Rev Cancer. 2012;12:323-34.

28. Stoecklein NH, Klein CA. Genetic disparity between primary tumours, disseminated tumour cells, and manifest metastasis. International Journal of Cancer. 2010;126:589-98.

29. Klein CA. Parallel progression of primary tumours and metastases. Nat Rev Cancer.

2009;9:302-12.

30. Chen ZY, Zhong WZ, Zhang XC, Su J, Yang XN, Chen ZH, et al. EGFR mutation heterogeneity and the mixed response to EGFR tyrosine kinase inhibitors of lung adenocarcinomas. The oncologist. 2012;17:978-85.

31. Chicklore S, Goh V, Siddique M, Roy A, Marsden PK, Cook GJ. Quantifying tumour heterogeneity in 18F-FDG PET/CT imaging by texture analysis. Eur J Nucl Med Mol Imaging. 2013;40:133-40.

32. Cook GJ, Yip C, Siddique M, Goh V, Chicklore S, Roy A, et al. Are pretreatment 18F-FDG PET tumor textural features in non-small cell lung cancer associated with response and survival after chemoradiotherapy? J Nucl Med. 2013;54:19-26.

33. Hong R, Halama J, Bova D, Sethi A, Emami B. Correlation of PET standard uptake value and CT window-level thresholds for target delineation in CT-based radiation treatment planning. International journal of radiation oncology, biology, physics. 2007;67:720-6.

34. Larson SM, Erdi Y, Akhurst T, Mazumdar M, Macapinlac HA, Finn RD, et al. Tumor Treatment Response Based on Visual and Quantitative Changes in Global Tumor Glycolysis Using PET-FDG Imaging: The Visual Response Score and the Change in Total Lesion Glycolysis. Clinical Positron Imaging. 1999;2:159-71.

35. Eisenhauer EA, Therasse P, Bogaerts J, Schwartz LH, Sargent D, Ford R, et al. New response evaluation criteria in solid tumours: Revised RECIST guideline (version 1.1). European Journal of Cancer. 2009;45:228-47.

36. Amadasun M, King R. Textural features corresponding to textural properties. Systems, Man and Cybernetics, IEEE Transactions on. 1989;19:1264-74.

37. Fang YH, Lin CY, Shih MJ, Wang HM, Ho TY, Liao CT, et al. Development and evaluation of an open-source software package "CGITA" for quantifying tumor heterogeneity with molecular images. BioMed research international. 2014;2014:248505.

38. Ho KC, Fang YD, Chung HW, Liu YC, Chang JW, Hou MM, et al. TLG-S criteria are superior to both EORTC and PERCIST for predicting outcomes in patients with metastatic lung adenocarcinoma treated with erlotinib. Eur J Nucl Med Mol Imaging. 2016;43:2155-65.

39. Fogelman I. The flare phenomenon: still learning after 35 years. European Journal of Nuclear Medicine and Molecular Imaging. 2011;38:5-6.

40. Krupitskaya Y, Eslamy HK, Nguyen DD, Kumar A, Wakelee HA. Osteoblastic Bone Flare on F18-FDG PET in Non-small Cell Lung Cancer (NSCLC) Patients Receiving Bevacizumab in Addition to Standard Chemotherapy. Journal of Thoracic Oncology. 2009;4:429-31.

41. Al-Nabhani K, Syed R, Haroon A, Almukhailed O, Bomanji J. Flare response versus disease progression in patients with non-small cell lung cancer. Journal of radiology case reports. 2012;6:34-42.

42. Jamal-Hanjani M, Quezada SA, Larkin J, Swanton C. Translational Implications of Tumor Heterogeneity. Clinical Cancer Research. 2015;21:1258-66.

43. Yatabe Y, Matsuo K, Mitsudomi T. Heterogeneous distribution of EGFR mutations is extremely rare in lung adenocarcinoma. J Clin Oncol. 2011;29:2972-7.

44. Vignot S, Frampton GM, Soria JC, Yelensky R, Commo F, Brambilla C, et al. Next-generation sequencing reveals high concordance of recurrent somatic alterations between primary tumor and metastases from patients with non-small-cell lung cancer. J Clin Oncol. 2013;31:2167-72.

45. Thomas A, Rajan A, Lopez-Chavez A, Wang Y, Giaccone G. From targets to targeted therapies and molecular profiling in non-small cell lung carcinoma. Annals of Oncology. 2013;24:577-85.

46. Taniguchi K, Okami J, Kodama K, Higashiyama M, Kato K. Intratumor heterogeneity of epidermal growth factor receptor mutations in lung cancer and its correlation to the response
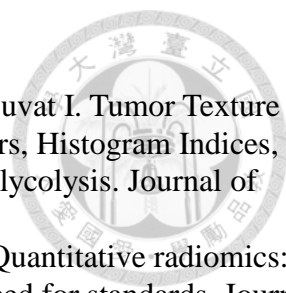
to gefitinib. Cancer science. 2008;99:929-35.

47. Orlhac F, Soussan M, Maisonobe J-A, Garcia CA, Vanderlinden B, Buvat I. Tumor Texture Analysis in 18F-FDG PET: Relationships Between Texture Parameters, Histogram Indices, Standardized Uptake Values, Metabolic Volumes, and Total Lesion Glycolysis. Journal of Nuclear Medicine. 2014;55:414-22.

48. Nyflot MJ, Yang F, Byrd D, Bowen SR, Sandison GA, Kinahan PE. Quantitative radiomics: impact of stochastic effects on textural feature analysis implies the need for standards. Journal of medical imaging. 2015;2:041002.